Proc. Natl. Acad. Sci. USA
Vol. 89, pp. 8547–8551, September 1992
Neurobiology

Dynamic surrounds of receptive fields in primate striate cortex: A physiological basis for perceptual completion?

(monkey/visual cortex/receptive-field structure/optic disk/visual psychophysics)

MARIO FIORANI, JR.*†, MARCELLO G. P. ROSA*‡, RICARDO GATTASS*§,
AND CARLOS EDUARDO ROCHA-MIRANDA*

*Departamento de Neurobiologia, Instituto de Biofísica Carlos Chagas Filho, Universidade Federal do Rio de Janeiro, Rio de Janeiro RJ 21941, Brazil; and §Laboratory of Neuropsychology, National Institute of Mental Health, Bethesda, MD 20892

Communicated by Mortimer Mishkin, June 11, 1992 (received for review March 20, 1992)

ABSTRACT **Visual receptive fields (RFs) were mapped inside and outside the cortical representation of the optic disk in the striate cortex (area V1) of anesthetized and paralyzed *Cebus* monkeys. Unexpectedly, most cells were found to be binocularly driven, and the RFs mapped with contralateral-eye stimulation progressed in a topographically appropriate fashion as the optic disk sector was crossed. Activation of these neurons by the contralateral eye was shown to depend on stimulation of the parts of the retina around the optic disk. Outside the optic disk representation, a similar effect was demonstrated by obstructing the "classical" RF with masks 5–10 times larger in size. In all cases, visual stimuli presented around the mask could be used to accurately interpolate the position of the hidden RF. These properties reflect, at a cellular level, the process of "filling in" that allows for completion of the visual image across natural and artificially induced scotomas.**

In the past decade, the notion that receptive fields (RFs) in adult sensory cortex have stable boundaries was challenged by a series of experiments that demonstrated changes in RF size and location after chronic (1–3) or acute (4) deafferentation. In the visual cortex, similar modifications have been seen after retinal lesions (5–7). In addition, even in the normal animal the portion of the visual field capable of modifying cellular activity has been shown to be far more extensive than the "classical" RF. Specifically, responses to stimulation within RFs of neurons in primate visual areas V1, V2, V3A, V4, and MT are modifiable by stimulation of normally silent RF peripheries with patterns differing in texture, wavelength, spatial frequency, direction of motion, and speed of motion from the pattern presented to the RF itself (6, 8–13). Responses in area V2 can be induced by illusory contours formed by visual patterns presented outside the classical RF (14) and the boundaries of excitatory RFs in area V4 vary depending on spatial attention (15). Except for the modulation of responses by stimulation of silent peripheries with patterns differing in speed of motion (6), most of these effects seemed to be absent in the primary visual area (V1), thus contributing to the hypothesis that RFs of neurons in V1 have stable boundaries and responses.

The retinal blind spot, corresponding to the optic disk, is devoid of photoreceptors. Thus, although most parts of the central visual field are usually viewed binocularly, the parts corresponding to the optic disk of one eye are viewed only through the opposite eye. Nonetheless, unless specific tests are applied, no gap in the visual field is noticed under monocular viewing. The blind spot is imperceptibly "filled in" to match the color, texture, and brightness of the regions of the visual field immediately surrounding the optic disk (16). This process of filling in is usually referred to as the completion phenomenon (16, 17). This phenomenon may also account for the unawareness of other "blind" regions of the retina, such as those overlaid by large retinal vessels (angioscotomata, ref. 18) and those produced by retinal lesions or lesions in the visual pathway (19, 20).

We report on a multi- and single-unit analysis of the visual responses of neurons in the parts of area V1 corresponding to the natural and artificially produced blind regions. We provide evidence that neurons within the cortical representation of the optic disk can interpolate RF position based on the stimuli that extend beyond the boundaries of the blind sector. These properties therefore mirror, at a cellular level, the perceptual completion phenomenon. Moreover, we show that the ability to interpolate RF position across large distances is also present in neurons in other parts of V1 as well. In these neurons, masking of the classical RF uncovers further excitatory regions that increase the effective excitatory RF length by up to 10 times. A preliminary report on these data was published in abstract (21).

MATERIALS AND METHODS

Multi- and single-unit responses were recorded from area V1 in four adult monkeys (*Cebus apella*). A detailed description of the animal preparation and recording procedures has been published (22). Briefly, at least 1 week before the first recording session the animal was anesthetized with ketamine (30 mg/kg) and Saffan and surgically implanted with a cranial prosthesis capable of holding the head in a modified stereotaxic holder without further pressure points. Recording sessions were subsequently carried out twice a week. During the sessions, the animals were anesthetized with nitrous oxide/oxygen, 7:3, paralyzed with a continuous infusion of pancuronium bromide (0.1 mg/kg per hr), and artificially ventilated through a tracheal cannula. Electrocardiogram, body temperature, and end-tidal CO_2 values were continuously monitored and kept within the physiological range. After 6–8 hr of recording the infusion of pancuronium was discontinued, and the animal was returned to its cage after recovering spontaneous breathing and consciousness.

Recordings were made by using varnish-coated tungsten microelectrodes inserted through the dura mater. Three-hundred twenty-eight multi-unit (MU) recordings were used to map the representation of the visual field in the cortex, and 165 single-unit recordings were used for quantitative analysis of RF properties in V1. The borders and the centers of the

The publication costs of this article were defrayed in part by page charge payment. This article must therefore be hereby marked "*advertisement*" in accordance with 18 U.S.C. §1734 solely to indicate this fact.

Abbreviations: MU, multi-unit; RF, receptive field; MURF, MU RF; PSTH, peristimulus–time histogram; V1, primary visual cortex.

†To whom reprint requests should be addressed.
‡Present address: Vision, Touch and Hearing Research Centre, University of Queensland, QLD 4072, Australia.

MU RF (MURF) were mapped for each eye at every 50–100 μm along each penetration passing close to the optic disk representation in V1. Single neurons isolated with an amplitude-waveform discriminator were continuously monitored with a Nihon–Koden (V10) memory oscilloscope. Using oriented bars, we first determined the orientation selectivity and ocular dominance of each single unit. Using a personal computer-based data-acquisition system, we then constructed peristimulus–time histograms (PSTHs) to flashing and moving bars with and without neutral masks of various sizes placed on the back of the tangent screen centered on the RF geometrical center. Size and location of the RFs were determined with PSTHs to long bars in the optimal and orthogonal to the optimal orientations, moving at different position offsets relative to the RF center. The trial-by-trial single-unit data were used to perform the quantitative analysis illustrated in Figs. 3 and 4. Outlines of the optic disks were mapped at the beginning of the session by using a reversible ophthalmoscope. To monitor position of the eyes during the experiment, a small mirror (0.5-mm diameter) was glued to the rim of hard contact lenses used to focus the eyes on the surface of the tangent screen. The mirror was used to reflect a low-intensity laser beam onto the surface of a screen. Position of the laser source was kept constant, and the lenses were allowed to attach to the cornea by the drying lachrymal film. Thirty minutes later, any eye movement clearly displaced the laser reflection on the screen. Eye position was routinely checked at the beginning and end of each quantitative analysis and each penetration. Three types of stimuli were used: three-dimensional bars, rear-projected stimuli, and computer-generated stimuli. Initially, characteristics of the responses and visual topography of MU clusters and cells in the optic disk representation were qualitatively evaluated by presenting long, opaque-colored bars on the surface of a transparent hemispheric screen. The qualitative evaluation was followed by quantitative analysis of single-unit response properties with the personal computer-based data-acquisition system. In most experiments we used a computer-driven optical bench that presented black-and-white bars and edges onto a Polacoat tangent screen located 1.14 m from the animal. In later experiments, a 48-cm Super VGA color monitor driven by a graphic board was used instead. Stimulus illumination was set at 22.6 cd/m^2, and background was set at 10.8 cd/m^2. A low contrast was deliberately chosen to reduce possible effects of stray light. Masking was achieved by inserting opaque gray cardboard squares of several sizes, which covered the classical RF as well as neighboring parts of the visual field. Data from 43 single neurons that had complete sets of histograms for both eyes, for different mask sizes, and for bars of different sizes and locations were used for statistical analysis (*t* test).

After 3 weeks of recordings, the animals were monocularly enucleated under ketamine/Saffan anesthesia. A survival time of 18 days was allowed before perfusion. All monkeys were perfused with 3% (wt/vol) paraformaldehyde/phosphate-buffered saline, and every section was treated for cytochrome oxidase (23) to reveal the limits of the cortical optic disk representation (22), the electrode tracks, and the electrolytic lesions (4 μA, 5 sec) used as markers.

RESULTS

Dimensions of the optic disk in the *Cebus* monkey average 6.0° × 4.5° of the visual field (24), whereas MURFs at a similar eccentricity (15°) seldom exceed 2–3° per side in area V1 (25). We, therefore, expected that tangential penetrations crossing the cortical representation of the optic disk in V1 would yield sites responsive only to the stimulation of the ipsilateral eye and that the boundaries of the blind region could be mapped in detail. Instead, by using long bars as stimuli and MU recordings, we found that most sites responded to both eyes and that a visual topography was preserved, even for the eye contralateral to the hemisphere under study (Fig. 1), in spite of the absence of photoreceptors in this part of the retina. However, the responses elicited by stimulation of the ipsilateral eye were invariably stronger, and the progression of contralateral-eye RFs showed a larger degree of scatter. Surprised by these observations, we decided to test (*i*) whether the same phenomenon could be observed at the single-unit level, and (*ii*) whether the contralateral responses could be due to the stimulation of regions of the visual field remote from the RF itself, in the manner illustrated in Fig. 2. Fig. 2*A* shows that sweeping bars longer than the diameter of the optic disk induced responses along restricted portions of the visual space (stars). In poorly oriented units, the location of the excitatory regions defined an interpolated RF (shown in black). In orientation-selective units, only RF width could be defined. Masking of the whole OD with opaque cardboard changed neither location of the interpolated RF nor strength of the responses (Fig. 2*B*). Sweeping bars restricted to one side of the OD (Fig. 2*C*) yielded either poor responses or no activation at all in some of these neurons, hereafter called completion neurons. In other units, the sum of the responses to separate stimulation of each side of the optic disk was comparable to the response elicited by a full bar, indicating the existence of a discontinuous RF for the contralateral eye. As detailed below, these two kinds of responses seen in the natural blind spot may not necessarily indicate the existence of separate classes of cells because some units behaved in either way, depending on the extent of an artificial, mask-induced blind region. Finally, a large mask covering the surround of the optic disk, but leaving the optic disk itself uncovered, abolished the responses (Fig. 2*D*). These tests argue against stray light as a source of artifact. In general, these observations reveal the

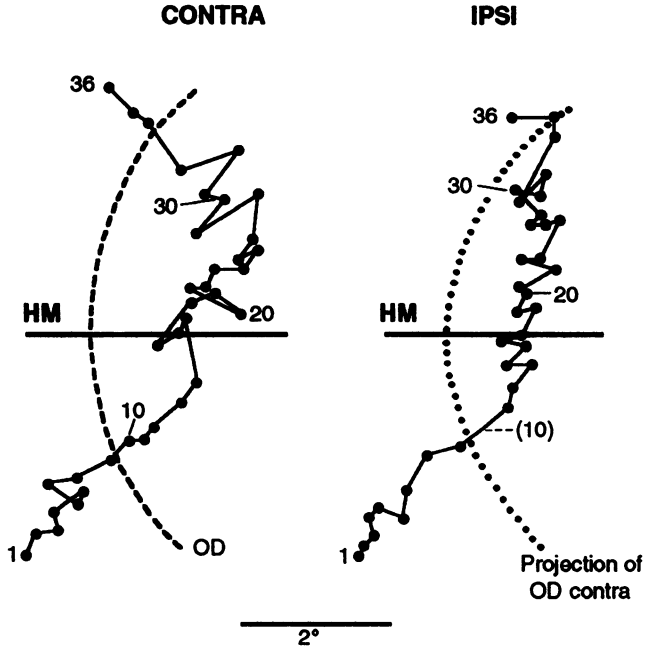

FIG. 1. Location of ipsilateral eye MURF centers (*Right*) and contralateral eye interpolated MURF centers (*Left*) recorded along a tangential penetration through the roof of the calcarine sulcus. Nasal limits of the projection of the optic disk (OD) in the visual field are shown by dashed lines, and the corresponding part of the visual field of the opposite eye is shown in small dots. Numbers indicate RFs for each eye recorded in sites 50–100 μm apart. Site 10 yielded responses to the contralateral eye only. HM, horizontal meridian; IPSI and CONTRA refer to the eye ipsi- and contralateral to the hemisphere under study, respectively.

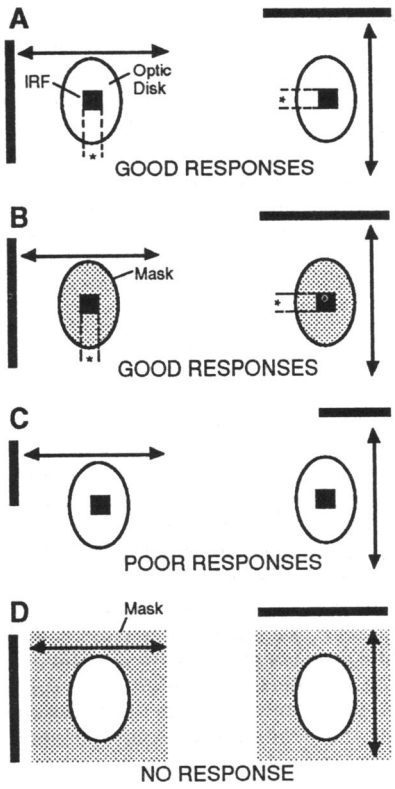

FIG. 2. Summary of neuronal responses (*A–D*) in the optic disk representation to oriented bars (left, vertical; right, horizontal) and masks of different shapes (*B*, *D*). Stars and dashed lines indicate locations where stimulation with long bars elicited responses. Stipples indicate masked regions, and arrows indicate direction of motion of oriented bars (shown in black). IRF, interpolated RF (black squares).

ability of V1 neurons to interpolate RF position in a blind region based on stimulation of regions of the visual field remote from the RF itself, hereafter referred to as dynamic surrounds.

Fig. 3*A* illustrates the responses of a cell located in layer IVb inside the histologically reconstructed optic disk representation. The mean response rate is shown for each eye separately as a function of size of the natural and mask-induced blind regions. In every test, a sweeping bar protruded at least 10° beyond the mask. Length of the classically mapped RF of this cell for the ipsilateral eye, based on measurements taken from PSTHs, was ≈1° (white arrowhead). Nonetheless, this unit responded well above spontaneous activity under contralateral-eye stimulation when the natural blind spot was left uncovered (far left). Adding square masks up to 15° per side still did not prevent this cell from responding, provided that coherent motion between the two protruding bar tips was achieved (Fig. 3*B*). Noteworthy is the fact that a reversal in the ocular dominance of the cell is apparent as larger masks are added. Although the responses to the ipsilateral eye are more than twice as strong as the interpolated contralateral responses in the mask-free condition, the interposition of masks 7.5° or more per side reveals a stronger response for the contralateral eye, and for masks beyond 12.5° per side only a contralateral response is apparent. Thus, the ocular dominance of the dynamic surround does not necessarily follow that of the classical RF. This unit showed above-background contralateral-eye responses to half-bar stimulation of either side of the optic disk in the mask-free condition (data not shown), thus qualifying as having a "discontinuous RF" property. However, Fig. 3*B* shows that when larger masks were used, a true completion

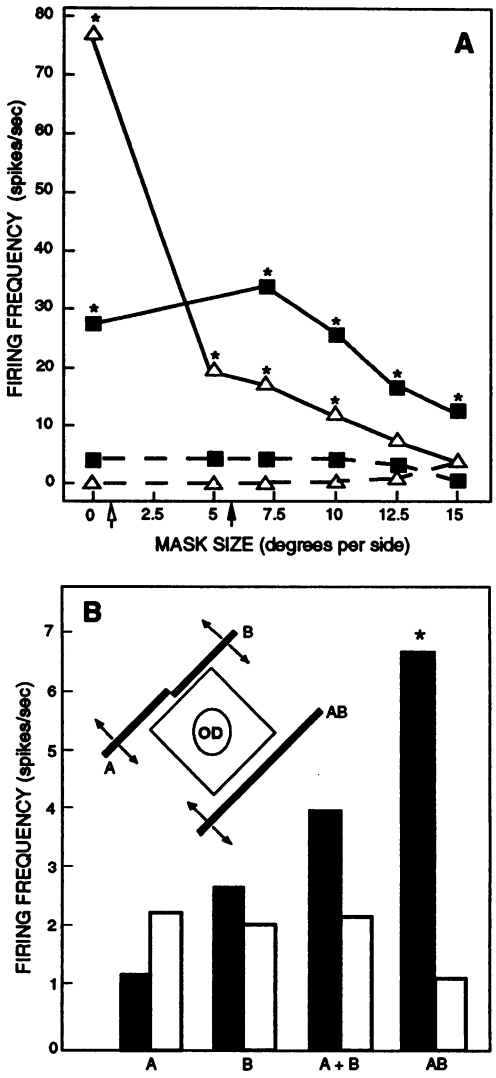

FIG. 3. (*A*) Mean response rate of a V1 cell for 10 presentations of the stimulus under different masking conditions. △—△, ■—■, Responses to ipsilateral and contralateral eye, respectively, in paired trials. The lower (dashed) lines show the mean spontaneous activity when each eye is opened separately. Size of the ipsilateral classical RF is shown by an outlined arrow, and the diameter of the optic disk is shown by a filled arrow. (*B*) Black bars show the mean response frequency of the same neuron to stimulation over a mask 15° per side; open bars show the mean spontaneous activity in paired trials without stimulation. The sum (bars A+B) of the activities to the presentation of partial slits (bars A or B) is smaller than the magnitude of the response to a full slit (bars AB). OD, optic disk. Stars indicate above-background activity ($P < 0.01$).

property was revealed. This specific cell was sharply tuned for orientation, and the orientation selectivity curves for the classical RF (mapped through ipsilateral-eye stimulation) and of the interpolated RF (mapped through the contralateral eye) showed similarly located peaks and bandwidths. Nine out of 43 single neurons had interpolated RFs inside the blind spot, and 4 out of 9 single neurons showed completion properties.

Fig. 4 shows response properties of a single neuron with poor orientation selectivity for which the RF was located at 14° eccentricity in the lower visual field away from the optic disk. PSTHs are shown for moving bars in the best (horizontal PSTHs) and orthogonal (vertical PSTHs) stimulus orientations. In spite of the restricted RF dimensions (stippled squares at upper left, based on the response envelopes in the no mask condition), the cell responded significantly when masks up to 10° per side were used. The largest mask

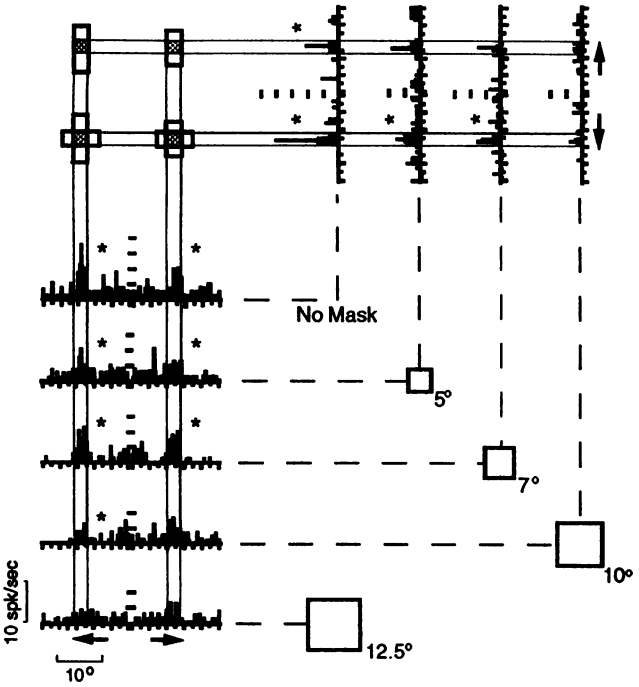

FIG. 4. PSTHs recorded from a V1 neuron with poor orientation selectivity in several masking conditions. Mask sizes (in degrees per side) used in each condition are shown in the appropriate scale at lower right; the RF (stippled) and length of the effective dynamic surround (rectangles) are shown in the same scale at upper left. ★, Significant above-background responses ($P < 0.01$).

size that allowed a significant response is shown for each combination of orientation and direction of motion in the upper left diagram (outlined rectangles). Although the interpolated RF profile is nearly constant, the extent of the previously silent region in which stimulation can drive interpolation (dynamic surround) varies according to the stimulation parameters. Fig. 5 compares the sizes of classical unitary RFs in *Cebus* monkeys (present results) and macaque monkeys (26–29) with the extent of the dynamic surrounds we observed. RF sizes in V1 of *Cebus* resemble those of macaques. The inclusion of dynamic surrounds as parts of the

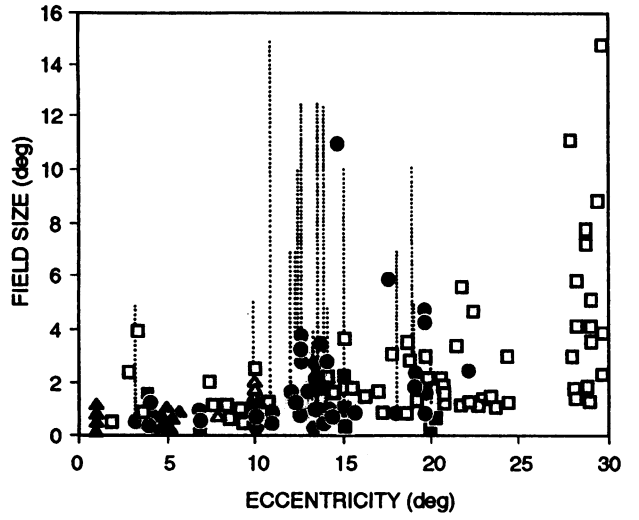

FIG. 5. RF size as function of eccentricity in *Cebus* (●) and macaque (□, ■, △, ▲). ·····, Size of dynamic surrounds of several units from *Cebus* monkeys; △, data from Hubel and Wiesel (26); ▲, data from Hubel and Wiesel (27); □, data from Zeki (28); and ■, data from Schiller *et al.* (29).

RFs reveals, however, that neuronal activity can be driven by far more extensive regions of the visual field.

Fifteen out of 43 single neurons in V1 were characterized as capable of interpolation across a region of the visual field at least three times as long as the classical RF width. Although the sample is too small to draw firm conclusions about their laminar distribution, completion neurons were found, with one exception, only in layers IVc-α, IVb, and VI, intermixed with other units without responses beyond the classical RF. A single completion neuron was found in layer III.

DISCUSSION

We report on a previously undescribed property of single neurons in the primary visual cortex of monkeys. Briefly, masking the classical excitatory RF uncovers further excitatory regions that may increase the RF areas as much as 100 times. Moreover, this increment in the excitatory RF size is accomplished without any loss of retinotopic order because the information obtained by stimulation of the RF active surround can be used to accurately interpolate the original position of the RF center. Two types of properties were described. (*i*) Some cells responded to the stimulation of both sides of a blind or masked region (discontinuous RFs). (*ii*) In some instances (especially when large masks were used), a coherent stimulation of both sides of the masked region was necessary for the excitation of some neurons (completion neurons). Discontinuous RFs have been reported (5, 7) to occur at the boundary of lesion-induced scotomas and the present results show the existence of such fields around the representation of the optic disk. Both discontinuous RF and completion properties were often seen in the same neurons, and these properties may both contribute to override the interference produced by natural and artificial scotomas.

Methodological Considerations. Two possible sources of artifact that could account for the above observations are stimulation of the classical RF by stray light and eye movements. The latter was excluded by the induction of neuromuscular paralysis and by a careful monitoring of eye position during the experiment. At the doses of pancuronium we used, the only movement seen was a very slow drift of the eyes, seldom exceeding 1–2° during the entire experiment. This fact was taken into account in our estimates of the limits of the optic disk during each trial. With regard to stray light, we find it unlikely to be a source of error because stimulus contrast was kept low and because completion neurons and neurons with discontinuous RFs responded to dark bars in light background as well as to the reverse contrast. Moreover, in several penetrations these neurons were found among units in the same portion of the visual field that did not respond outside the classical RF.

We determined the maximum extent of the dynamic surrounds with long bars moving across the visual field and a series of masks with increased dimensions. This method is appropriate to determine the extent of the surround, but it does not assess the contribution of the surround to the classical RF response in the absence of the masks. Adaptation or conditioning experiments are necessary to determine the interactions between the response of a neuron to its surrounds and the classical RF properties of a neuron.

Completion Phenomenon. The ability to interpolate image features in the absence of direct stimulation based on regions of the visual field remote from the RF suggests an analogy with the perceptual completion phenomenon, in which images across naturally blind regions of the retina, such as the optic disk, are filled in. Existence of such neurons in all portions of V1 up to 20° eccentricity (the region covered by our recordings) could contribute to image continuity, overriding the interference of blood vessels (18) or the presence

of other natural or lesion-induced scotomas (19, 20). The procedure of masking the visual field around a RF has obvious and important qualitative differences from using a region naturally devoid of photoreceptors, but in the present study both procedures yielded comparable results. In a paralyzed preparation, such as the one we used, any static boundary (as the border of the masks) will gradually fade, and the corresponding portion of the visual field will be filled in by the pattern in the background (17). Absence of visual input generated inside the masked region may be regarded as qualitatively similar to that generated by a lesion either in the retina or in the visual pathways and, therefore, filled in by a similar process. The interpolation responses seem to represent a mechanism different from that demonstrated by Peterhans and von der Heydt (14) for illusory contour-driven activity in neurons in V2. Interpolation responses occur over a much wider area of the visual field than do illusory contour-driven responses, and these former responses are present in area V1, which lacks the local mechanism described by Peterhans and von der Heydt for V2. Moreover, on psychophysical grounds, illusory contours are apparent, even when the subject is free to move its eyes, whereas completion requires steady fixation or image stabilization. We hypothesize that the properties described here are relevant for completion but not to the perception of illusory contours, which may rely on activity of extrastriate neurons. In addition, our findings indicate that perceptual completion may rely on activity at the level of single neurons in the primary visual cortex.

Possible Sources of the Interpolation Response. The large extent of the dynamic surrounds and the restricted arborization of geniculostriate fibers (27) make it unlikely that this pathway alone is responsible for generating interpolation responses. At an eccentricity of 15°, the cortical magnification factor of V1 of *Cebus* is ≈0.7 mm per degree (25), and, therefore, to overcome the gap generated by a mask 15° per side, portions of V1 more than 5 mm away would have to send inputs to the completion neuron (7.5° to each side). Intrinsic connections of monkey striate cortex are reported to span several millimeters (30), and the longest intrinsic axons may have the necessary coverage for generating long-range interpolations. In a recent study, Gilbert and Wiesel (7) observed acute and chronic changes in RF position and extent after retinal lesions and attributed such changes to the intrinsic connections of V1. In this context, the dynamic unmasking of active surrounds seen in these experiments indicates that even under normal physiological conditions these intrinsic connections may contribute to the delineation of RF extent. Some of the largest RFs recorded in V1, specifically those from layer VI, approach the size of the dynamic surrounds (Fig. 5) and, therefore, may contribute to generating the completion responses in the upper layers. Alternatively, the massive extrastriate feedback projections to striate cortex (31) could be important in generating interpolation responses. Neuronal RFs in areas such as MT and V4 are normally similar in size to the dynamic surrounds of V1 neurons at comparable eccentricities and, therefore, can integrate information across much larger portions of the visual field.

We thank Drs. Mortimer Mishkin, Michael Calford, Aglai P. B. Sousa, and Robert Desimone for helpful comments on the manuscript. Financial support was from Conselho Nacional de Desenvolvimento Científico e Tecnológico (CNPq), Financiadora de Estudos e Projetos (FINEP), and Fundação de Amparo à Pesquisa do Estado do Rio de Janeiro (FAPERJ).

1. Rasmusson, D. D. (1982) *J. Comp. Neurol.* **205,** 313–326.
2. Merzenich, M. M., Kaas, J. H., Wall, J. T., Sur, M. & Felleman, D. J. (1983) *Neuroscience* **10,** 639–665.
3. Pons, T. P., Garraghty, P. E., Ommaya, A. K., Kaas, J. H., Taub, E. & Mishkin, M. (1991) *Science* **252,** 1857–1860.
4. Calford, M. B. & Tweedale, R. (1988) *Nature (London)* **332,** 446–448.
5. Kaas, J. H., Krubitzer, L. A., Chino, Y. M., Langston, A. L., Polley, E. H. & Blair, N. (1990) *Science* **248,** 229–231.
6. Heinen, S. J. & Skavenski, A. A. (1991) *Exp. Brain Res.* **83,** 670–674.
7. Gilbert, C. D. & Wiesel, T. N. (1992) *Nature (London)* **356,** 150–152.
8. Zeki, S. M. (1983) *Neuroscience* **9,** 767–781.
9. Allman, J. M., Miezin, F. & McGuiness, E. (1985) *Annu. Rev. Neurosci.* **8,** 407–430.
10. Tanaka, K., Hikosaka, K., Saito, H., Yukie, M., Fukada, Y. & Iwai, E. (1986) *J. Neurosci.* **6,** 134–144.
11. Desimone, R. & Schein, S. J. (1987) *J. Neurophysiol.* **57,** 835–867.
12. Allman, J. M. (1990) in *Signal and Sense: Local and Global Order in Perceptual Maps*, eds. Eldeman, G. M., Gall, C. M. & Cowan, M. (Wiley-Liss, New York) pp. 131–141.
13. Gaska, J. P., Jacobson, L. D. & Pollen, D. A. (1988) *Vision Res.* **27,** 1687–1692.
14. Peterhans, E. & von der Heydt, R. (1989) *J. Neurosci.* **9,** 1749–1763.
15. Moran, J. & Desimone, R. (1985) *Science* **229,** 782–784.
16. Helmholtz, H. (1963) *Handbook of Physiological Optics* (Optical Soc. of America, Dover, DE).
17. Ramachandran, V. S. & Gregory, R. L. (1991) *Nature (London)* **350,** 699–702.
18. Le Grand, Y. (1967) *Form and Space Vision* (Indiana Univ. Press, Bloomington).
19. Bender, M. B. & Teuber, H. L. (1946) *Arch. Neurol. Psychiatry* **55,** 627–658.
20. Weiskrantz, L. (1986) *Blindsight, A Case Study and Implications* (Oxford Psychology Series, Oxford).
21. Fiorani, M., Jr., Gattass, R., Rosa, M. G. P. & Rocha-Miranda, C. E. (1990) *Soc. Neurosci. Abstr.* **16,** 1219.
22. Rosa, M. G. P., Gattass, R., Fiorani, M., Jr., & Soares, J. G. M. (1992) *Exp. Brain Res.* **88,** 249–264.
23. Wong-Riley, M. T. T. (1979) *Brain Res.* **171,** 11–28.
24. Rosa, M. G. P., Gattass, R. & Fiorani, M., Jr. (1988) *Exp. Brain Res.* **72,** 645–648.
25. Gattass, R., Sousa, A. P. B. & Rosa, M. G. P. (1987) *J. Comp. Neurol.* **259,** 529–548.
26. Hubel, D. H. & Wiesel, T. N. (1968) *J. Physiol. (London)* **195,** 215–243.
27. Hubel, D. H. & Wiesel, T. N. (1974) *J. Comp. Neurol.* **158,** 295–306.
28. Zeki, S. M. (1983) *Proc. R. Soc. London B* **217,** 449–470.
29. Schiller, P. H., Finlay, B. L. & Volman, S. F. (1976) *J. Neurophysiol.* **39,** 1288–1319.
30. Rockland, K. S. & Lund, S. J. (1983) *J. Comp. Neurol.* **216,** 303–318.
31. Sousa, A. P. B., Pinon, M. C. G. P., Gattass, R. & Rosa, M. G. P. (1991) *J. Comp. Neurol.* **308,** 665–682.